

Foaming behavior of water-soluble cellulose derivatives: hydroxypropyl methylcellulose and ethyl hydroxyethyl cellulose

Kristina Karlsson · Erich Schuster ·
Mats Stading · Mikael Rigdahl

Received: 24 March 2015 / Accepted: 21 May 2015 / Published online: 27 May 2015
© Springer Science+Business Media Dordrecht 2015

Abstract Hydroxypropyl methylcellulose and ethyl hydroxyethyl cellulose could be interesting candidates for production of lightweight, foamed packaging material originating from non-fossil, renewable resources. The foaming ability of nine different grades of the two cellulose derivatives, using water as the blowing agent, was investigated using a hot-mold process. The foaming process was studied by evaluating the water loss during the heating, both in a real-time experiment and by thermal gravimetric analysis. Further, the development of the rheological properties of the derivative-water mixtures during a simulated foaming process was assessed using dynamical mechanical thermal analysis and viscosity measurements. Five of the studied derivatives showed promising properties for hot-mold foaming and the final foams were characterized with regard to their apparent density. It was concluded that the foamability of these systems seems to require a rather careful tailoring of the viscoelastic properties in relation to the water content in order to ensure that a network structure is built up and expanded during the water evaporation.

Keywords Cellulose derivatives · Hydroxypropyl methylcellulose (HPMC) · Ethyl hydroxyethyl cellulose (EHEC) · Foaming · Rheological characterization · Bulk density

Introduction

The industrial demand for cheap, lightweight, disposable packaging materials has led to an extensive use of fossil-based polymeric foams such as expanded polystyrene (EPS) and polyurethane (PU) foams. In 2010 the global production of PUs was about 14 million tonnes and about three quarters of this was in the form of foams (Quadrini et al 2013). In 2012 the global polymeric foam market was worth about 82.6 billion US dollars and there is an expected growth of about 7.7 % yearly from 2013 onwards (Folkesson 2014). However, these materials have two major drawbacks. The first one regards the raw material originating from a non-renewable resource and the second one is the often difficult, uneconomical recycling and the slow degradation of these foams in nature (Hofer 2008). This has created a need for a light, cheap accessible and sustainable alternative.

The challenge of finding a material that can compete pricewise and without exhibiting inferior mechanical properties compared to the fossil-based foams remains. One promising candidate raw material is cellulose from wood. Cellulose is both abundant and renewable. Cellulose fibers have previously been used

K. Karlsson (✉) · M. Stading · M. Rigdahl
Department of Materials and Manufacturing Technology,
Chalmers University of Technology, 41296 Gothenburg,
Sweden
e-mail: kristina.karlsson@chalmers.se

E. Schuster · M. Stading
SP - Food and Biotechnology, 40229 Gothenburg, Sweden

as reinforcing elements in biopolymer foams (Svagan et al. 2011) and the mechanical properties of nanofibrillar cellulose foams have also been studied (Ali and Gibson 2013). Bacterial cellulose has been used, with good result, to reinforce and improve the properties of foamed cassava-starch trays (da Silva et al 2013). Cellulose has also been used as filler to reduce the cost of extruded acetylated starch foams (Guan and Hanna 2006).

Cellulose consists of long polysaccharide chains, structurally consisting of a linear homopolymer backbone, formed by D-glucopyranose units linked by β -1–4 glycosidic bonds, which varies in length but can be up to 15,000 monomer units long. As pure cellulose is insoluble in water, different chemical modifications are needed in order to tailor the properties of cellulose to suit some applications (Klemm et al. 2005; O'Sullivan 1997). Especially water-soluble cellulose derivatives are widely used in industrial applications e.g. in foods, pharmaceuticals and paints, where they are used as thickeners, binding agents, emulsifiers, surfactants, lubricants and stabilizers (Clasen and Kulicke 2001). Such water-soluble cellulose derivatives result from the substitution of hydroxyl groups in each anhydroglucose ring by hydroxypropyl and methyl groups in the case of hydroxypropyl methylcellulose (HPMC) and ethyl and hydroxyethyl groups are attached to the anhydroglucose units by ether linkages in the case of ethyl hydroxyethyl cellulose (EHEC). Such functional groups decrease the crystallinity of the substance and hence increase the solubility in water.

Here, the possibility to foam HPMC and EHEC using a hot-mold process was investigated. Water was used as both blowing agent and plasticizer. The foaming ability of five different grades of HPMC and four different grades of EHEC was evaluated using different polymer concentrations and foaming temperatures. The different grades varied, and were selected with regard to molecular weight or averaged substitution pattern to evaluate their respective effect on foaming.

Similar techniques have previously been used to produce starch foams (Uslu and Polat 2012; Shogren et al. 1998; Kaewtatip et al. 2014) and water together with microfibrillated cellulose has been reported as a successful blowing agent for poly(lactic acid) (Boisard et al. 2011). Foams based on cellulose derivatives have previously been produced using e.g. cellulose acetate with azodicarbonamide as blowing agent and

also from biodegradable cellulose acetate butyrate (CAB) using supercritical carbon dioxide (scCO₂) as blowing agent (Deanin and Bernier 1996; Kemmere et al. 2008).

In order to understand the foaming ability and the related mechanisms the rheological behavior of the water-polymer solutions was investigated. The molding process and the water loss were studied using thermal gravimetric analysis (TGA) and dynamic mechanical thermal analysis (DMTA). The produced foams were characterized with regard to their apparent densities and by scanning electron microscopy (SEM) imaging.

Experimental

Materials

HPMC grades of different solution viscosities (corresponding to different molecular weights) and substitution patterns from Shin-Etsu Chemical Co. (Tokyo, Japan) were used, see Table 1 for details. EHEC was kindly supplied by AkzoNobel, see Table 2 for more details about the samples. The data in Tables 1 and 2 were provided by the suppliers.

Methods

Preparation of foams

The polymer in powder form was dissolved in water using an 80 °C water bath and a magnetic stirrer. The solution was then poured into circular aluminum foil molds (diameter of 27 mm) in a double hot-plated baking machine (Franz Haas Waffelmaschinen, Austria). The temperature was set to 160–180 °C depending on the concentration of the sample and the molding times varied between 8 and 10 min. A slight pressure was applied from the weight of the top plate upon closing of the mold. The water evaporated and acted as a blowing agent for the foaming. The foams were let to cool and stored at 50 % relative humidity and 20 °C, until further analyses were conducted.

Estimation of water loss during foaming

In order to estimate the water loss during the foaming process, the hot mold was placed on a scale (Mettler

Table 1 Compilation of tested HPMC samples

| Sample | Abbreviation | Viscosity (mPa·s) ^a | Methoxy content (%) | Hydroxypropoxyl content (%) |
|---------------------|--------------|--------------------------------|---------------------|-----------------------------|
| HPMC Metolose/60SH | HPMC60-50 | 50 | 28.0–30.0 | 7.0–12.0 |
| HPMC Metolose/60SH | HPMC60-4000 | 4000 | 28.0–30.0 | 7.0–12.0 |
| HPMC Metolose/65SH | HPMC65-4000 | 4000 | 27.0–30.0 | 4.0–7.5 |
| HPMC Methocel/K4MCR | HPMCK4-4000 | 4000 | 19.0–24.0 | 7.0–12.0 |
| HPMC Metolose/60SH | HPMC60-10000 | 10,000 | 28.0–30.0 | 7.0–12.0 |

^a 2 wt % aqueous solution at 20 °C according to the USP measuring method. According to Shin-Etsu Chemical co. <http://www.metolose.jp/e/pharmaceutical/metolose.shtml>

Table 2 Compilation of tested EHEC samples. DS-degree of substitution, the number of hydroxyl groups per 1,4-anhydroglucose unit that have reacted. MS-molecular substitution, the average total number of ethylene oxide groups per 1,4-anhydroglucose unit. HM-hydrophobically modified, M-methyl

| Sample | Name/abbreviation | Viscosity (mPa·s) | DS-ethyl | DS-methyl | MS-ethylene oxide |
|---------|-------------------|------------------------|----------|-----------|-------------------|
| EHEC | E230FQ | 260–360 ^a | 0.8–1.0 | – | 1.8–2.5 |
| EHEC | E351FQ | 5000–6000 ^a | 0.8–1.0 | – | 1.8–2.5 |
| HM-EHEC | EHM200 | 350–700 ^b | 0.8–1.0 | – | 1.8–2.5 |
| MEHEC | M10 | 750–1000 ^c | 0.2–0.3 | 0.7–1.3 | 0.3–1.2 |

^a 2 wt % aqueous solution at 20 °C with Brookfield viscometer type LV at speed of 12 rpm

^b 1 wt % aqueous solution at 20 °C with Brookfield viscometer type LV at speed of 12 rpm

^c Information provided by supplier

Toledo IND226) with an accuracy of 1 g. A digital probe thermometer (Testo 735) was placed in the polymer solution and the temperature and the weight were manually recorded with 10 s intervals during the entire foaming process.

Thermal gravimetric analysis of the water loss

TGA was employed in order to obtain a more detailed picture of the water loss during heating. The polymer solution was placed in the measuring cup and the TGA instrument (Pyris, TGA7) recorded the weight loss due to evaporation of the water as a result of increasing temperature in air atmosphere. The experiments were performed at two different temperature rates, 5 °C/min and 16 °C/min, and the weight loss was assumed to correspond only to water evaporation (no degradation).

Dynamic mechanical thermal analysis

The foaming process was simulated with DMTA, which is a well-known tool for characterizing the

viscoelastic properties of materials. The aim was to assess the hardening (stiffness increase) of the material, as the water evaporated due to the temperature increase. Here, 0.5 g of 10 wt% HPMC-50 was inserted between the plates of the DMTA instrument (Rheometrics Scientific RSA-II) which were enclosed by an oven. The bottom plate was flat and circular and larger than the 15 mm diameter top plate in order to eliminate any confinement effects from the edges. Temperature ramps from 40 to 220 °C at a rate of 5 °C/min were applied, in which the top plate was following the surface of the expanding sample by keeping a constant load of 0.15 N, and hence measuring the change in sample height during the process. The viscoelastic properties, i.e. the storage modulus E' and the loss modulus E'' , were evaluated as a function of temperature by applying a periodic compression deformation of 1 Hz and an amplitude of 0.05 % (within the linear viscoelastic regime). This analysis was only performed on the HPMC polymer solutions.

Changes in the complex viscosity as well as in the shear storage and loss moduli due to an increase in

temperature were also studied using a strain-controlled rheometer (TA Instruments ARES-G2) with a 40 mm diameter parallel plate geometry. The samples were heated from 22 to 92 °C (HPMC) and 22 to 100 °C (EHEC) at a rate of 5 °C/min. Paraffin oil was added to the periphery of the sample to prevent it from drying during heating. These oscillatory measurements were carried out at 1 Hz and 0.1 % strain amplitude. Note that in this case the position of the upper plate of the rheometer was kept constant, i.e. it did not follow the expansion of the foaming material.

Shear viscosity at room temperature

The viscosity of the HPMC-solutions was determined at room temperature using a strain-controlled rheometer (TA Instruments ARES-G2) with a 40 mm diameter parallel plate geometry. If possible, the samples were tested both in the shear and the oscillatory mode. For samples of higher polymer concentration only the oscillatory mode was used and the complex viscosities as a function of angular frequency are reported. The Cox-Merz rule (Cox and Merz 1958) was assumed to apply.

Density

The density of the foams was determined gravimetrically and with volume approximations using a sand displacement method similar to the one used by Sjöqvist (Sjöqvist and Gatenholm 2007). Each foam was cut into 4 mm slices using a surgical stainless steel blade and at least four slices per foam sample were used. A Mettler Toledo AG285 balance was used to determine the weight. The foam slices were then immersed in sand in a 10 ml measuring cylinder until completely covered, the glass was tapped for 1 min and the difference in volume was recorded. The foam density was calculated as the measured weight divided by the approximated volume.

Scanning electron microscopy (SEM)

A scanning electron microscope (DSM940A, ZEISS Germany) was used to study the pore structure of the foams. Thin slices were cut from the foams using a surgical stainless steel blade and these were then glued, using carbon glue, onto aluminum stubs. The samples were sputter coated with gold (S150B

Edwards Sputter Coater) for 1 min under vacuum and thin carbon glue lines were made to connect the conducting surfaces. Both the top surfaces as well as the cross-sections of three different samples were studied.

Results

Production of foams

Out of the nine derivatives that were tested five of them produced porous foams within certain polymer concentration, temperature and processing time ranges. When starting the foamability studies, a concentration of 10 wt% was chosen as a reference point. Then the concentration range was extended (if considered being of interest). Table 3 summarizes the results from the foaming trials. HPMC60-10000 showed a tendency for foaming, but only at polymer concentrations too low to give a stable foam, i.e. the cells were large and the cell walls very thin. The same applied (weak foams) to HPMC60-4000 foamed at 150 °C at a concentration of 3 wt%. The visually best foams were obtained with HPMCK4-4000 (5 % and 190 °C), HPMC60-4000 (5 % and 170 °C) and HPMC60-50 (10 % and 170 °C). In general, all of the HPMCs, possibly with exception of the grade with the highest molecular weight, exhibited a good foamability (depending on the foaming conditions), whereas only one of the EHECs, the methyl-substituted, did.

Estimation of water loss during foaming

In order to obtain an improved understanding and characterization of the foaming process the water loss of the samples during the molding process was recorded manually. Both the decrease in weight and the temperature of the polymer solution/foam was measured as a function of time. The gravimetric measurement is admittedly rather crude due to the accuracy of the balance used, but the primary aim was to obtain an indication of the course of events during the foaming. An example of the weight and temperature development during the process is given in Fig. 1 in case of HPMC60-50. The molding temperature was 180 °C and the initial polymer concentration 10 wt%. The measurements (as function of

Table 3 Summary of the foaming results obtained with the hot-molding process

| Sample | Viscosity (mPa·s) | Foams (Y/N) ^a | Concentration (%) | Temperature range (°C) | Time in mold (min) |
|---------------|-------------------|--------------------------|-------------------|------------------------|--------------------|
| HPMC60-50 | 50 | Y | 10 | 160–200 | 7–12 |
| | | | 15 | 160–200 | |
| | | | 20 | 160–210 | |
| | | | 25 | 160–220 | |
| HPMC60-4000 | 4000 | Y | 3 ^b | 140–190 | 8–10 |
| | | | 5 | 145–180 | |
| | | | 10 | 160–200 | |
| HPMC65-4000 | 4000 | Y | 10 | 165–180 | 8–12 |
| HPMCK4-4000 | 4000 | Y | 5 | 140–190 | 8–10 |
| | | | 8 | 150–180 | |
| | | | 10 | 150–200 | |
| HPMC60-10,000 | 10,000 | b | 3–5 | 170 | 8–12 |
| M10 | 750–1000 | Y | 5 | 160 | 8–11 |
| | | | 10 | 140–170 | |
| E230FQ | 260–360 | N | 10 | 160–170 | 8–9 |
| EHM200 | 350–700 | N | 10 | 160 | 8 |
| E351FQ | 5000–6000 | N | 10 | 160 | 8 |

^a Y = yes/N = no

^b Weak foam

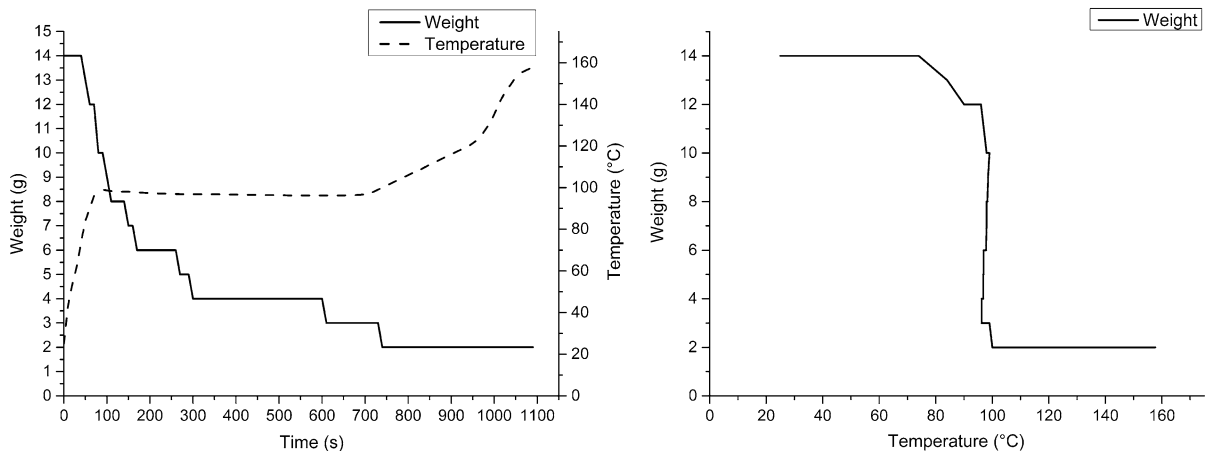


Fig. 1 Left The water loss (full line) and the temperature (dashed line) of the polymer solution as a function of time. Right The relation between the weight loss and the temperature. The

polymer used was HPMC60-50 with a concentration of 10 wt%. The molding temperature was 180 °C

time) can be combined to give the relation between weight loss and temperature, see Fig. 1. Since the cellulose derivatives used are expected to degrade less than 20 % at temperatures below 306 °C (Prasad et al. 2008), the weight loss is assumed to correspond only

to the water loss. Note that in the molding process, the polymer solution is immediately exposed to a high mold temperature.

The final temperature of the foamed sample was measured to be approximately 160 °C which means

that the temperature increased from 22 to 160 °C in approximately 18 min. This gives an average temperature increase of about 7.5 °C/min.

As expected, the temperature increase was not linear over time (Fig. 1, left). Within the first 70 s the temperature reached a plateau just below 100 °C, where the main part of the water evaporation retarded a further temperature increase for about 11 min before the temperature increased again. After this evaporation phase, the temperature increased about 60 °C during the remaining 6 min; here giving a rate of about 10 °C/min. Thus, even though the polymeric water-containing sample was placed on the 180 °C hot plate, the temperature response was in a sense quite slow.

The experiment described above was repeated several times, with different starting weights of the samples and slightly different plate temperatures for different polymers. However, the pattern of the evaporation was quite similar for all samples.

Thermal gravimetric analysis of the water loss and viscoelastic characterization of the foaming process

In order to obtain a more controlled measurement of the weight loss as the temperature increases and to monitor the conditions at hand during foaming in the rheological equipment (described later), TGA experiments were performed. Figure 2 shows the result from the TGA measurement performed at a polymer concentration of 10 % HPMC60-50. Two different heating rates were used; 5 and 16 °C/min, the former used to model the foaming in the rheometer and the later the foaming in the hot mold.

The foaming process was further simulated using DMTA by following the development of the viscoelastic properties in compression of the material during foaming as well as the geometric expansion over time. In order to visualize the different states of HPMC60-50 (10 wt%) during foaming one measurement was carried out in which the oven of the rheometer was opened and a series of images were taken at every 10 °C increase. Figure 3 displays the most important events.

The sample was a transparent and rather viscous fluid up to about 70 °C. At this temperature, some cloudiness could be seen and at about 80 °C the sample turned quite white. At 100 °C small bubbles became visible and at 120 °C the porous structure was

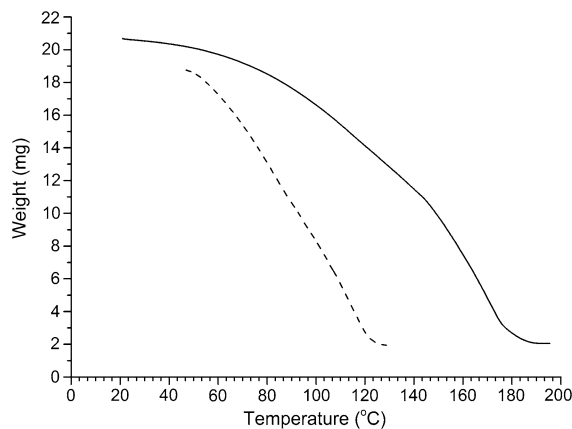


Fig. 2 TGA curves displaying the weight loss of 10 % HPMC60-50 as a function of the temperature. *Full line:* 16 °C/min, *dashed line:* 5 °C/min

clearly evident. Between 120 and 150 °C the white color faded as the foam structure dried and stabilized. Above 160 °C some degradation may take place since the foam became somewhat brownish at the edges. The behavior described here can be said to be quite typical for the HPMCs used. The methyl-substituted EHEC (M10) was the only one of the EHECs used that exhibited a foaming ability. In fact, this polymer behaved quite similar to the HPMCs, i.e. a clouding was observed at higher temperatures followed by an expansion.

The corresponding changes in the viscoelastic properties of HPMC60-50 (initial concentration 10 %) are illustrated in Fig. 4. At lower temperatures, below 70 °C, the loss modulus (E'') was higher than the storage modulus (E') meaning that viscous effects are dominating in this region. At about 70 °C a crossover can be seen and the elastic component was from now on larger than the viscous. Shortly after the crossover a steep increase of the moduli followed. This increase flattened out just above 100 °C and may partly be associated with difficulties in obtaining accurate data in this region of excessive water evaporation. At about 120 °C the moduli increased further and reached a maximum around 150–160 °C. At higher temperature, the moduli decreased which may not be surprising. Figure 4 also shows the vertical movement of top plate of the rheometer, which corresponds to the expansion in millimeters of the produced foam. As evident, the major expansion was initiated at temperatures slightly higher than 100 °C and a maximum was obtained at around 120 °C. After

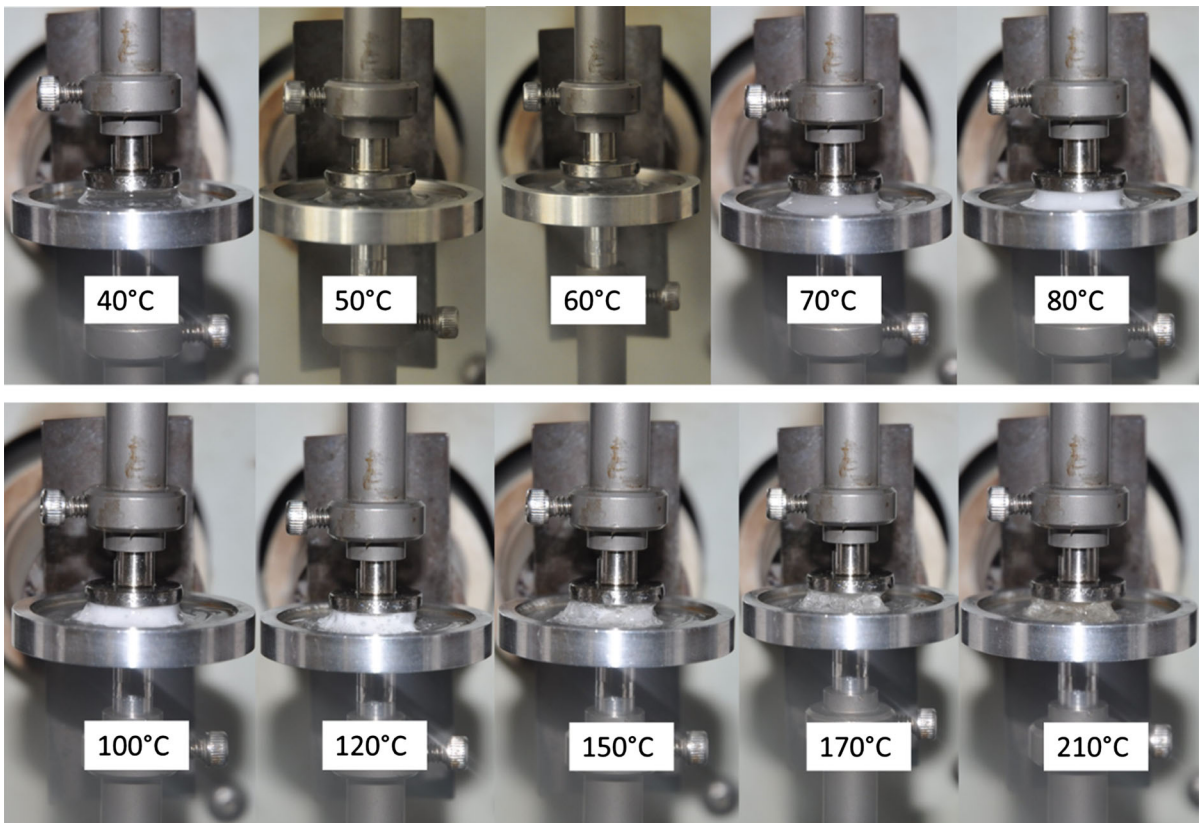
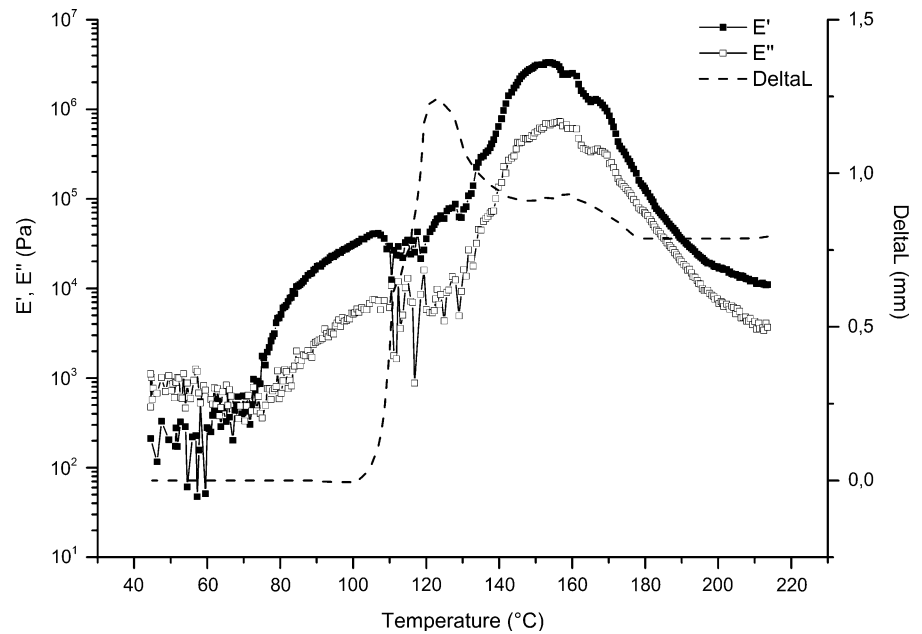


Fig. 3 Visualization of a dynamic temperature ramp test, 5 °C/min, 40–210 °C during foaming of HPMC60-50, 10 wt%

Fig. 4 Dynamic temperature ramp test, 5 °C/min, 40–220 °C, showing loss (E'' , open squares) and storage (E' , full squares) modulus in Pascal and the expansion (DeltaL, dashed line) in millimeters as a function of temperature during foaming of HPMC60-50, 10 %



some shrinkage at higher temperatures, the height increase seemed to stabilize around 0.75–0.80 mm.

Note that the absolute values of the moduli in Fig. 4 should be viewed with some caution, since the dimensions of the specimen changed during the foaming and squeeze flow may occur during the early stages. From Figs. 3 and 4, important transitions temperatures are suggested as; cloud point between 60–70 °C, crossover at 70 °C and the midpoint of the steep increase in modulus at about 85 °C. Note that the crossover of E' and E'' have been suggested to correspond to the formation of a physical gel (Tung and Dynes 1982; Winter and Chambon 1986).

Rheological characterization of the polymer solutions/foams

In order to obtain some insight into the rheological prerequisites for the ability of the solutions to foam and form stable foams, further studies of the rheological behavior were undertaken.

Shear viscosity and flow behavior at room temperature

Figure 5 displays the shear viscosity and the shear stress as a function of shear rate for HPMC60-50 at increasing polymer concentrations and at room temperature. As expected, the viscosity increased with increasing concentration and the non-Newtonian character also became more evident.

Figure 6 shows the corresponding viscosity results for one of the polymers (EHM200) that did not produce a stable foam structure during the molding process. The polymer concentration was 5, 10 or 15 wt %. In this case, the measurements had to be carried out in the oscillatory mode due to the initially high viscosity of the solution.

Compared to HPMC60-50 (Fig. 5), the viscosities of the EHM200-solutions were significantly higher at the same polymer concentration and the shear-thinning was also more pronounced. For example, at 5 % polymer content HPMC60-50 had a viscosity of about 1 Pa·s at a shear rate of 0.1 s^{-1} whereas for EHM200 the corresponding viscosity at the same concentration was about 400 Pa·s. It was not possible to measure the viscosity when the concentration of EHM200 was 20 %.

The storage and loss moduli are also included in Fig. 6. Both the viscosity and the moduli increased

strongly with increasing polymer concentration. Note that except at the lowest polymer concentration and at very low frequencies, the storage modulus of EHM200 was always higher than the loss modulus.

The temperature dependence of the viscoelastic properties of HPMC60-50 and EHM200

The moduli of HPMC60-50 and EHM200 are shown as functions of the temperature in Fig. 7. The polymer concentration was 5 % in both cases. As already evident from Fig. 4, the moduli of the HPMC sample increased with increasing temperature whereas for the EHEC sample, the moduli decreased up to approximately 80 °C and then went through a minimum. Further, for HPMC G'' is higher at low temperatures and the moduli exhibit a crossover between 40 and 50 °C, whereas for EHM200 $G' > G''$ in the entire investigated temperature region, i.e. up to 100 °C.

As noted earlier, the loss modulus of the HPMC sample, G'' , was higher than the storage modulus, G' , at lower temperatures. Upon increasing the temperature the behavior of the material undergoes a change from exhibiting a softer, more viscous response to a harder, more elastic one. In case of the EHEC sample, the storage modulus was higher than the loss modulus in the whole temperature range used. It is noteworthy that the moduli of EHM200 were significantly higher than those of the HPMC60-50 at lower temperatures, i.e. prior to the initiation of the foaming. The decrease in moduli in case of EHM200 is consistent with a thermal softening of the material. The increase in the viscoelastic properties at higher temperatures could possibly be due to experimental set-up, i.e. the fixed top plate in the rheometer. Another possible explanation for the increase could be an effect from the edges which were observed to dry up and harden somewhat due to water evaporation, even when the protective oil was used, during heating. This could affect the measurements of the moduli.

Comparing Figs. 4 and 7 (right) for HPMC60-50, a similar qualitative course of events are noted, but the absolute values of the moduli differ somewhat. The primary reason for this is believed to be associated with the different geometrical set-ups. Figure 4 refers to measurements where the upper plate followed the expansion of the material, whereas in Fig. 7 the results were obtained with the upper plate in a fixed position.

Fig. 5 Shear viscosity (*full symbols*) and shear stress (*open symbols*) as a function of the shear rate at different concentrations (5–20 %) of HPMC60-50 at 22 °C and a relative humidity of 47 %

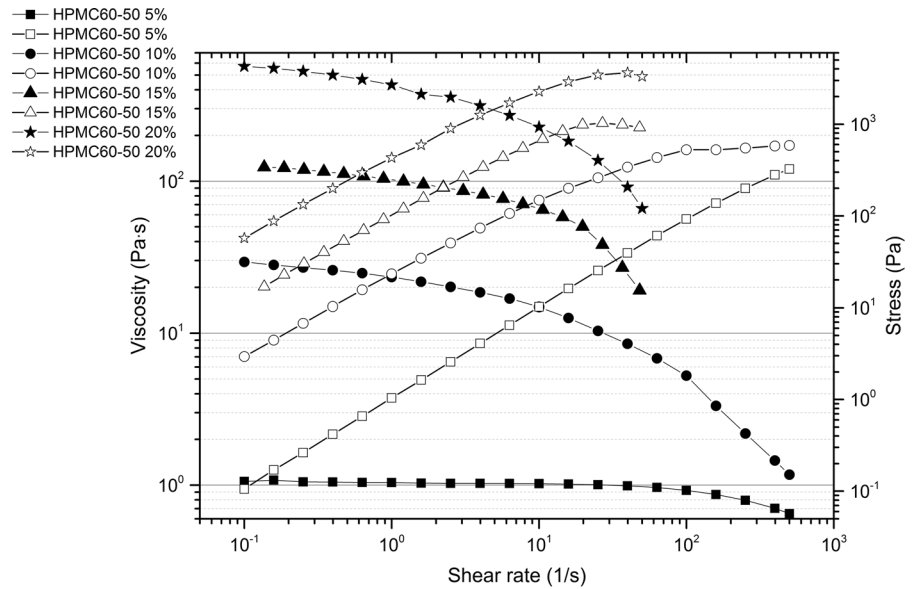
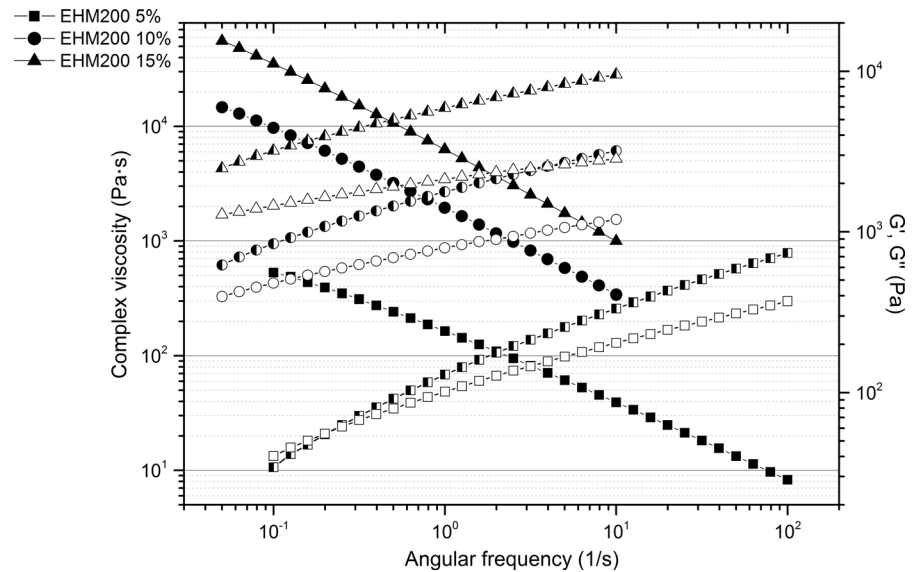


Fig. 6 The complex viscosity (*full symbols*), the storage modulus (*half symbols*) and the loss modulus (*open symbols*) as a function of the angular frequency at increasing concentrations (5–15 %) of EHM200. The measurements were performed at room temperature (22 °C)



Scanning electron microscopy

Scanning electron microscopy (SEM) was performed in order to visualize the internal and the surface structure of some of the foamed samples. In total six different samples from two different types of HPMCs were studied. The top images in Fig. 8 show SEM images from HPMC60-50 and the bottom two from HPMC60-4000. From the images it is clear that the samples contained a large number of pores of varying

size and shape. It can also be seen that the surfaces of the foams, i.e. the sides that were touching the plates during the foaming, had a different skin-like structure.

Apparent densities of the foams

Figure 9 shows the apparent densities of foams produced at different temperatures and initial polymer concentrations for four different grades of HPMC. The HPMC foams produced exhibited a range of densities

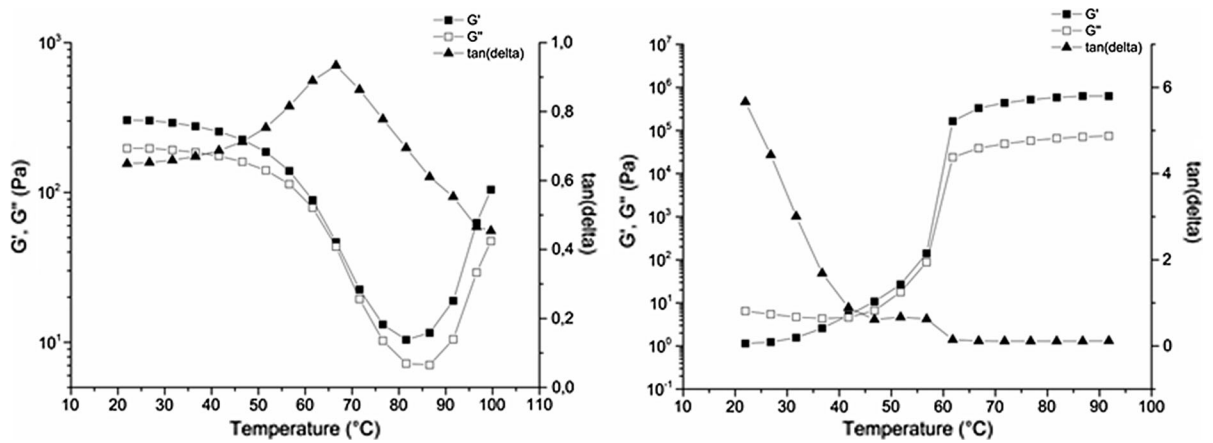


Fig. 7 The storage modulus (G' , full squares), the loss modulus (G'' , open squares) and $\tan(\delta)$ (full triangles) as a function of temperature. Left EHM200, 5 %. Right HPMC60-50, 5 %

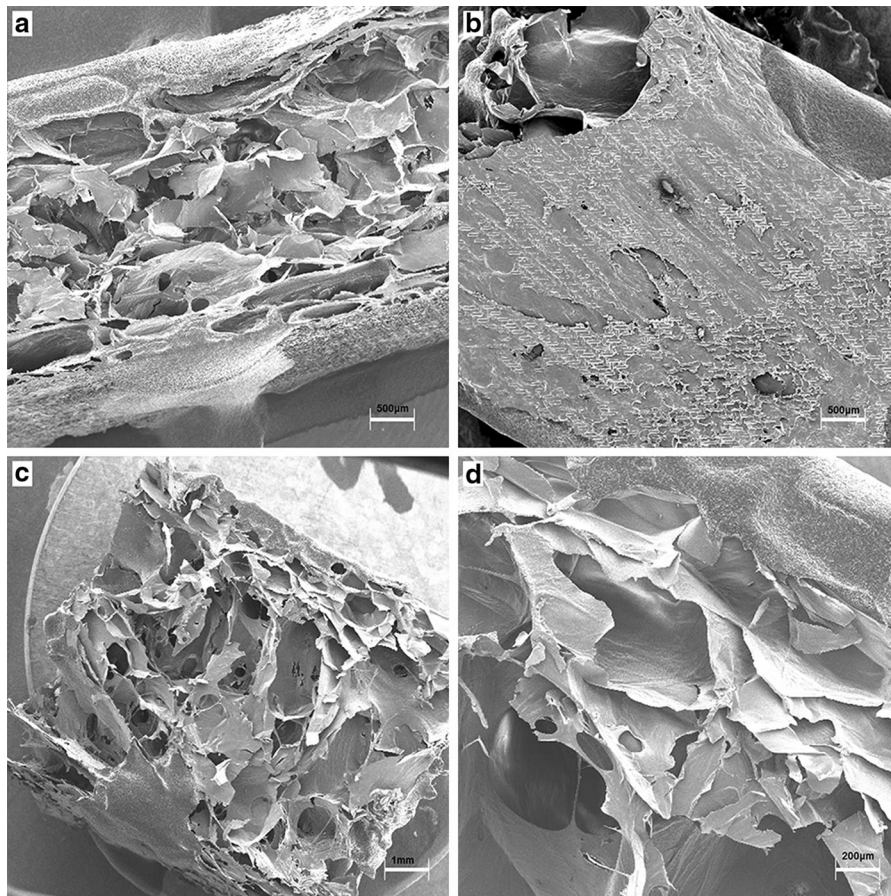
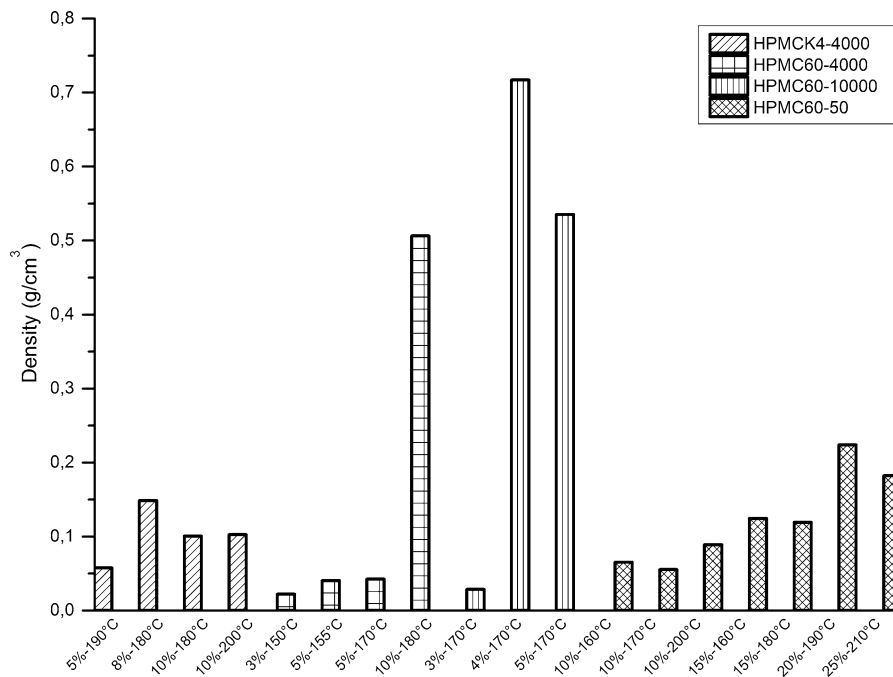


Fig. 8 a HPMC60-50, foaming temperature 160 °C, 10 %, cross-Section. b HPMC60-50, 160 °C, 10 %, surface view. c HPMC60-4000, 155 °C, 5 %, cross-Section. d HPMC60-4000, 155 °C, 5 %, cross-section

Fig. 9 Apparent densities of four different HPMC-samples. From left to right HPMCK4-4000, HPMC60-4000, HPMC60-10000, and HPMC60-50. The densities were measured on foams produced at different temperatures and initial concentrations



with values between 0.02 and 0.7 g/cm³. The most promising foams, i.e. stable structures with a low density, were obtained with HPMCK4-4000 (5 % and 190 °C), HPMC60-4000 (5 % and 170 °C) and HPMC60-50 (10 % and 170 °C).

Discussion

Water loss

As can be seen from Fig. 1 (left), most of the water evaporated close to 100 °C and above the water loss flattened out, which is not unexpected. Repeated weighing after the foam was taken out of the mold indicated that some minor amount of water still was present in the foam (<5 %). The rather crude measuring technique did however not allow for a more accurate determination. The limiting factor was clearly the scale which had to carry the weight of the hot mold but still be sensitive enough to record the change in sample weight in the mold. The scale had an accuracy of 1 g but with the weight of the machine on top the accuracy was reduced to about 2 g.

There was no direct correspondence between the weight loss curves in Fig. 1 and the results from the

TGA measurements, Fig. 2 (except for the fact that water evaporates rather quickly as the temperature approaches 100 °C). The time dependence of the water loss is obviously quite dependent on the heating rate. In the TGA equipment the specimens were heated at a controlled rate, whereas during the mold foaming they were immediately exposed to a hot environment leading to a faster water loss. In the mold the temperature rose from room temperature to 100 °C in about one minute. In the TGA the corresponding times were about 5 and 10 min at heating rates of 16 and 5 °C/min, respectively. The slower heating rate obviously gave more time for the sample to adapt to the surrounding temperature and more time for water to evaporate even before it reaches the boiling temperature. In line with this, Fig. 2 shows that at the lower heating rate (5 °C/min) almost all water had evaporated before the temperature exceeded 100 °C. It may also be pointed to that there was a substantial difference in sample weight between the two types of water loss experiments (about 10³ less material was used in the TGA) which can have a bearing on the kinetics of the weight loss.

What could be concluded from these studies is that the weight loss is probably quite fast in the molding

experiments and the major part of the water is evaporated around 100 °C.

Viscoelastic properties

HPMC is a cellulose derivative which exhibits thermal gelation properties. Starting with a HPMC solution at ambient temperature, increasing the temperature will lead to a phase separation commonly referred to as clouding. The initiation temperature varies depending on the substitution degree of the derivative and can be lowered by addition of salts (Allahbash et al. 2015). Hydrophobic interactions and hydrogen bonding lead upon further temperature increase to the build-up of an entangled three-dimensional network structure. At higher temperatures, this structure becomes stabilized and forms a strong gel; all considerations are still below 100 °C (Sekiguchi et al. 2003).

The transition temperatures noted here corresponds quite well with previously reported experimental results where the cloud point of HPMC K15 was found to be 68 °C and the crossover between G' and G'' at 72 °C for a 10 % polymer solution (da Silva et al. 2013). The present results indicate the cloud point to be between 60 and 70 °C and the crossover at 70 °C. The exact onset of clouding and gelation depends on the polymer concentration and substitution patterns (da Silva et al. 2013). Thermal degradation of HPMC starts only above 250 °C (Meena et al. 2014), thus the observed decrease in moduli and sample height at the end of the heating cycle (Fig. 4) is not due to degradation, but more likely due to stabilization of the foam and thermal softening. The DMTA experiments indicated a softening of the HPMC foam around 155 °C, in accordance with DSC data reported by (Meena et al. 2014) (McPhillips et al. 1999).

Greiderer et al. studied HPMC using reversed-phase liquid chromatography and aqueous size-exclusion chromatography and reported similar observations, namely an increasing hydrophobicity of the HPMC when temperature was increased (Greiderer et al. 2011). This increase in hydrophobicity initiated an aggregation of the polymer chains and led to the formation of a network structure which seems to be important for the foaming properties. Thus, for HPMC thermal gelation forms a stable network/matrix already below 100 °C, which seems favorable for foaming. This three-dimensional network structures prevails during the water evaporation at 100 °C and

builds the template for a foam. The foam expands as the water forms vapor and consolidates, provided that the stiffness and strength of the cell walls are sufficient, when the water has evaporated and the material is cooled below a specific softening point.

The EHEC and HM-EHEC samples showed no signs of thermal gelation behavior below 100 °C. Additionally the EHEC samples exhibited much higher viscosities and moduli than the HPMC systems at similar polymer concentrations. It could be that the generated steam pressure was not sufficient to expand this rather stiff and viscous polymer solution. Previous studies on the foaming ability of EHEC and sodium dodecyl sulphate (SDS) in aqueous solution in glass columns using nitrogen gas also showed no foam formation or stability for EHEC and water solution alone (Djuve et al. 2001). Thus the foamability seems to require a rather careful tailoring of the viscoelastic properties in relation to the water content in order to ensure that a network structure is built up and expanded during the water evaporation. A too high viscosity/modulus counteracts the blowing process and become unfavorable whereas a too low stiffness of the structure will result in a collapsed foam. Additionally a stabilization of the matrix during the foaming, possibly via thermal gelation, seems to be beneficial.

Apparent densities

Commercial polymeric foams such as EPS have a density of about 0.01–0.025 g/cm³ (Samper et al. 2010; Biron 2012) depending on production technique. For PU foams the apparent density is between 0.14 and 0.71 g/cm³ depending on the grade (Calvert et al. 2010). The cellulosic foams produced here had apparent densities between 0.02 and 0.7 g/cm³ thus comparable to that of existing commercial foams. It is clear that by optimizing the polymer concentration and the processing conditions HPMC foams with a suitable density can be produced.

Conclusion

The aim of this paper was to provide an improved understanding of alternative, renewable, materials which can be used in foaming applications and hopefully contribute to a reduction of the use of

fossil-based products in the future. In summary, we have here reported on the evaluation of renewable materials for foam production, the successful manufacturing of HPMC foams and the techniques used to study the foaming process. The first step was to evaluate which of the nine initial samples produced a stable foam structure in a hot mold forming process. Out of the nine samples six showed abilities to produce stable foam structures. The foamability (using water as the blowing agent) seems to require a rather careful tailoring of the viscoelastic properties in relation to the water content in order to ensure that a network structure is built up and expanded during the water evaporation. Further, the molecular weight of the polymer seems to influence the ability to foam (via the viscoelastic properties). High molecular weight HPMC did not produce foams with desirable densities for commercial comparison. Presumably, there is also a lower limit for chain length suitable for foaming. Such an investigation was however out of the scope of this paper.

Acknowledgments This work has been funded by The Swedish Research Council Formas who is greatly acknowledged for their contribution. Many thanks to AkzoNobel for material supply and valuable discussions. Further thanks to Anette Larsson, Gunnar Westman, Linda Hårdelin, Mikaela Börjesson and Marco Berta for interesting, helpful discussions about laboratory equipment and interpretation of results.

References

- Ali ZM, Gibson LJ (2013) The structure and mechanics of nanofibrillar cellulose foams. *Soft Matter* 9:1580–1588
- Allahbash S et al (2015) Interplay of thermal and covalent gelation of silanized hydroxypropyl methyl cellulose gels. *Carbohydr Polym* 115:510–515
- Biron M (2012) *Plastics design library: thermoplastics and thermoplastic composite*, 2nd edn. Elsevier Science, p 326
- Boissard CIR et al (2011) Water of functionalized microfibrillated cellulose as foaming agent for the elaboration of poly(lactic acid) biocomposites. *J Reinforced Plast Compos* 30(8):709–719
- Calvert K, Trumble K, Webster T, Kirkpatrick L (2010) Characterization of commercial rigid polyurethane foams used as bone analogs for implant testing. *J Mater Sci Mater Med* 21(5):1453–1461
- Clasen C, Kulicke W (2001) Determination of viscoelastic and rheo-optical material functions of water-soluble cellulose derivatives. *Prog Polym Sci* 26(9):1839–1919
- Cox WP, Merz EH (1958) Correlation of dynamic and steady flow viscosities. *J Polym Sci* 28(118):619–622
- da Silva A et al (2013) Cassava starch-based foams reinforced with bacterial cellulose. *J Appl Polym Sci* 130(5):3043–3049
- Deanin R, Bernier T (1996) Cellulose acetate structural foam. *J Vinyl Addit Technol* 2(3):263–264
- Djuve J, Pugh R, Sjoblom J (2001) Foaming and dynamic surface tension of aqueous polymer/surfactants solutions 1: ethyl(hydroxyethyl) cellulose and sodium dodecyl sulphate. *Colloids Surf A* 186(3):189–202
- Folkesson M (2014) Marknaden för polymerskum växer. *Plastforum*, 11 April, p 6. <http://www.plastnet.se/alla/marknaden-polymerskum-vaxer/>
- Greiderer A et al (2011) Characterization of hydroxypropylmethylcellulose (HPMC) using comprehensive two-dimensional liquid chromatography. *J Chromatogr A* 1218(34):5787–5793
- Guan J, Hanna MA (2006) Selected morphological and functional properties of extruded acetylated starch–cellulose foams. *Bioresour Technol* 97(14):1716–1726
- Hofer, T. N., 2008. Marine pollution: new research. *Nova Science Publishers*, p. 59
- Kaewtatip K, Pongroij M, Holló B, Mészáros Szécsényi K (2014) Effects of starch types on the properties of baked starch foams. *J Therm Anal Calorim* 115(1):833–840
- Kemmere M, Hurkens S, Keurentjes J, Jacobs L (2008) Porous cellulose acetate butyrate foams with a tunable bimodality in foam morphology produced with supercritical carbon dioxide. *Macromol Mater Eng* 293(4):298–302
- Klemm D, Heublein B, Fink H, Bohn A (2005) Cellulose: fascinating biopolymer and sustainable raw material. *Angewandte Chemie (International ed.in English)*, 44(22), pp 3358–3393
- McPhillips H, Craig DQM, Royall PG, Hill VL (1999) Characterisation of the glass transition of HPMC using modulated temperature differential scanning calorimetry. *Int J Pharm* 180(1):83–90
- Meena A, Parikh T, Gupta S, Serajuddin A (2014) Investigation of thermal and viscoelastic properties of polymers relevant to hot melt extrusion—II: cellulosic polymers. *J Excip Food Chem* 5(1):46–55
- O’Sullivan A (1997) Cellulose: the structure slowly unravels. *Cellulose* 4(3):173–207
- Prasad P, Guru GS, Shivakumar HR, Rai KS (2008) Miscibility, thermal, and mechanical studies of hydroxypropyl methylcellulose/pullulan blends. *J Appl Polym Sci* 110(1):444–452
- Quadrini F, Bellisario D, Santo L (2013) Recycling of thermoset polyurethane foams. *Polym Eng Sci* 53(7):1357–1363
- Samper M, Garcia-Sanoguera D, Parres F, Lopez J (2010) Recycling of expanded polystyrene from packaging. *Prog Rubber Plast Recycl Technol* 26(2):83–92
- Sekiguchi Y, Sawatari C, Kondo T (2003) A gelation mechanism depending on hydrogen bond formation in regioselectively substituted O-methylcelluloses. *Carbohydr Polym* 53(2):145–153
- Shogren RL, Lawton JW, Doane WM, Tiefenbacher KF (1998) Structure and morphology of baked starch foams. *Polymer* 39(25):6649–6655
- Sjöqvist M, Gatenholm P (2007) The effect of water content in potato amylopectin starch on microwave foaming process. *J Polym Environ* 15(1):43–50

- Svagan AJ, Berglund LA, Jensen P (2011) Cellulose nanocomposite biopolymer foam—hierarchical structure effects on energy absorption. *ACS Appl Mater Interfaces* 3:1411–1417
- Tung C, Dynes P (1982) Relationship between viscoelastic properties and gelation in thermosetting systems. *J Appl Polym Sci* 27(2):569–574
- Uslu M-K, Polat S (2012) Effects of glyoxal cross-linking on baked starch foam. *Carbohydr Polym* 87(3):1994–1999
- Winter H, Chambon F (1986) Analysis of linear viscoelasticity of a crosslinking polymer at the gel point. *J Rheol* 30(2):367–382